


Molecular Modeling and Bioinformatics Analysis of Drug-Receptor Interactions in the System Formed by Glargine, Its Metabolite M1, the Insulin Receptor, and the IGF1 Receptor

Bioinformatics and Biology Insights
Volume 15: 1–9
© The Author(s) 2021
Article reuse guidelines:
sagepub.com/journals-permissions
DOI: 10.1177/11779322211046403


Margarita González-Beltrán¹ and Claudio Gómez-Alegría² 

¹Grupo de investigación GRINCIBIO, Facultad de medicina, Universidad Antonio Nariño, Bogotá, Colombia. ²Grupo de investigación UNIMOL, Departamento de Farmacia, Facultad de Ciencias, Universidad Nacional de Colombia—Sede Bogotá, Bogotá, Colombia.

ABSTRACT

INTRODUCTION: Insulin and insulin-like growth factor type 1 (IGF1) regulate multiple physiological functions by acting on the insulin receptor (IR) and insulin-like growth factor type 1 receptor (IGF1R). The insulin analog glargine differs from insulin in three residues (Gly^{A21}, Arg^{B31}, Arg^{B32}), and it is converted to metabolite M1 (lacks residues Arg^{B31} and Arg^{B32}) by *in vivo* processing. It is known that activation of these receptors modulates pathways related to metabolism, cell division, and growth. Though, the structures and structural basis of the glargine interaction with these receptors are not known.

AIM: To generate predictive structural models, and to analyze the drug/receptor interactions in the system formed by glargine, its metabolite M1, IR, and IGF1R by using bioinformatics tools.

METHODS: Ligand/receptor models were built by homology modeling using SWISSMODEL, and surface interactions were analyzed using Discovery Studio® Visualizer. Target and hetero target sequences and appropriate template structures were used for modeling.

RESULTS: Our glargine/IR and metabolite M1/IR models showed an overall symmetric T-shaped conformation and full occupancy with four ligand molecules. The glargine/IR model revealed that the glargine residues Arg^{B31} and Arg^{B32} fit in a hydrophilic region formed by the α -chain C-terminal helix (α CT) and the cysteine-rich region (CR) domain of this receptor, close to the CR residues Arg270-Arg271-Gln272 and α CT residue Arg717. Regarding IGF1R, homologous ligand/receptor models were further built assuming that the receptor is in a symmetrical T-shaped conformation and is fully occupied with four ligand molecules, similar to what we described for IR. Our glargine/IGF1R model showed the interaction of the glargine residues Arg^{B31} and Arg^{B32} with Glu264 and Glu305 in the CR domain of IGF1R.

CONCLUSION: Using bioinformatics tools and predictive modeling, our study provides a better understanding of the glargine/receptor interactions.

KEYWORDS: Insulin glargine, insulin receptor, IGF type 1 receptor, receptor protein-tyrosine kinases, theoretical models, molecular models, protein conformation

RECEIVED: April 4, 2021. **ACCEPTED:** August 24, 2021.

TYPE: Original Research

FUNDING: The publication costs of this article were defrayed by the Fondo de fortalecimiento del grupo UNIMOL (Acta No. 013-2019).

DECLARATION OF CONFLICTING INTERESTS: The author(s) declared no potential conflicts of interest with respect to the research, authorship, and/or publication of this article.

CORRESPONDING AUTHOR: Claudio Gómez-Alegría, Grupo de investigación UNIMOL, Departamento de Farmacia, Facultad de Ciencias, Universidad Nacional de Colombia—Sede Bogotá, Cra 30 # 45-03, Ciudad Universitaria, Edificio 450, Código Postal 111321 Bogotá, Colombia. Email: cjomorza@unal.edu.co

Introduction

Insulin is a peptide hormone that plays a crucial role in physiology by regulating energy metabolism, cell growth, and differentiation.^{1,2} The mature hormone is composed of two peptide chains (chain A with 21 amino acids and chain B with 30 amino acids) held together by two disulfide bonds (Cys^{A7}-Cys^{B7}; Cys^{A20}-Cys^{B19}) and an additional intrachain-A disulfide bond (Cys^{A6}-Cys^{A11}).³⁻⁵ Insulin analogs are derived from human insulin by the substitution of certain amino acids, which generates molecules with different pharmacokinetic properties that are useful in diabetes management.⁶⁻⁸ One of these analogs is glargine, which differs from human insulin in three residues: glycine at A21 (Gly^{A21}) instead of asparagine, and two additional C-terminal arginine residues (Arg^{B31}, Arg^{B32}) in the

B-chain. These two new arginine residues change the isoelectric point thereby making this molecule less soluble at neutral pH; this leads to the formation of a subcutaneous microprecipitate where glargine is present as a hexamer that slowly dissociates and undergoes proteolysis, generating two main products referred to as metabolites M1 and M2,⁸⁻¹¹ with M1 being the physiologically more important metabolite.¹²

The metabolic effects of insulin and its analogs are mediated by IR, but glargine and other analogs also show mitogenic effects on cell cultures, which seems to be dependent on IGF1R.¹³⁻¹⁸ IR and IGF1R belong to the receptor tyrosine kinases superfamily (RTKs) encoded by 58 genes in humans.¹⁹ Both are part of the same RTK subfamily referred to as dimeric RTKs because they are expressed in cell membranes as dimers



of two covalently linked monomers either in the absence or presence of its ligands. Each monomer is composed of two covalently linked protein subunits: an extracellular ligand-binding α -subunit and a second membrane-bound β -subunit with an intracellular tyrosine kinase (TK) domain. Thus, these dimeric receptors $[(\alpha\beta)_2]$ are also considered as heterotetrameric proteins $(\alpha_2\beta_2)$.²⁰ IR and IGF1R share a common domain architecture: each extracellular (α) subunit is composed of two leucine-rich regions (L1 and L2) separated by a cysteine-rich region (CR), followed by two fibronectin type III domains (Fn-III1 and Fn-III2), an insert domain (ID α), and a C-terminal alpha helical segment (α CT); the β subunit has two type III fibronectin domains (Fn-III2 and Fn-III3), followed by an insert domain (ID β), a TM domain, and a tyrosine kinase (TK) domain, followed by a carboxyl terminal end.^{21,22} Despite their structural similarity, IR and IGF1R show functional divergence; IR is mainly involved in metabolic effects (by regulating carbohydrate, protein, and lipid metabolism), while IGF1R is mainly related to pathways that regulate growth, cell differentiation, and migration, which makes it a focus of interest for cancer-related studies.^{3,19,23} The activation mechanism of these receptors is triggered by ligand binding to the receptor ectodomain, followed by conformational changes that activate the intracellular TK domain and receptor auto-phosphorylation, which finally activates downstream signaling pathways that lead to their different effects.^{1,19}

The common architecture of IR and IGF1R, and the similarity between its ligands (insulin, IGF1, glargine, and its metabolites) seems to be the basis of the receptor promiscuity phenomenon observed in this protein receptor subfamily, in which different ligands can bind and activate the same receptor.^{5,24} Despite extensive knowledge of the pharmacokinetic properties of glargine and its analogs, little is known about the structural basis of the interaction between glargine or its metabolites with IR and IGF1R, because the structures of these complexes have not been solved so far. Here, bioinformatics tools were applied to propose hypothetical 3D structures of these ligand/receptor complexes, which revealed certain unknown structural aspects, such as the localization of the glargine residues ArgB31 and ArgB32 in these complexes.

Material and Methods

Homology modeling

The models were built using the SWISS-MODEL server.²⁵ For IR modeling (ectodomain) in complex with glargine (glargine/IR model) or its metabolite M1 (metabolite M1/IR model), we considered the proglargine sequence (74 amino acids) as our target sequence and the full-length IR sequence (1354 amino acids)²⁶ as the hetero target (see Supplementary Material S1 for this and all other sequences). The structure of the insulin-IR complex (PDB: 6PXV)²⁶ was selected as the template. The proglargine sequence consists of glargine

residues (chains A and B) separated by the first 21 residues of the proinsulin C-peptide (PDB: 6K59).²⁷ The inclusion of these 21 residues was necessary because any modeling attempt using only the glargine residues resulted in models that lacked the glargine A chain. In all our final models, the C-peptide residues were removed to obtain the glargine/IR (19 residues removed) and the metabolite M1/IR (21 residues removed) models. The residues were removed using Pymol (The PyMOL Molecular Graphics System, Version 2.0 Schrödinger, LLC). These models were then refined as described below. For insulin/IR modeling, proinsulin was used as the target sequence (74 amino acids)²⁶ and full-length IR (1354 amino acids) was used as the hetero target sequence. The insulin-IR complex reported by Uchikawa et al²⁶ (PDB: 6PXV) was selected as the template.

For IGF1R (ectodomain) modeling in complex with glargine and metabolite M1 as ligands, proglargine (110 amino acids) and full-length IGF1R (1367 amino acids) were used as the target and hetero target sequences, respectively (Supplementary Material S2).²⁸ As a template, two different cryo-electron microscopy (cryo-EM) structures were selected: IGF1R in complex with insulin (PDB: 6JK8)²⁸ and IR in complex with insulin (PDB: 6PXV).²⁶ As aforementioned, residues not belonging to glargine or metabolite M1 were removed from our models; after further refinement was performed as described below, our final glargine/IGF1R and metabolite M1/IGF1R models were obtained.

All the cryo-EM and crystallographic structures were obtained from the Protein Data Bank (<https://www.rcsb.org/>, 2021).²⁹

Refinement of the models

All the models were refined by removing the *random coil* regions of each receptor. Briefly, a superposition analysis between the theoretical model and the template structure was carried out using Discovery Studio® Visualizer (BIOVIA, Dassault Systèmes Discovery Studio Modeling Environment, Release 2017) by comparing the positions of the alpha carbons (C-alpha). Receptor regions involved in the ligand/receptor interactions in our model, but not well resolved in the crystal, were identified and removed with Pymol (The PyMOL Molecular Graphics System, Version 2.0 Schrödinger, LLC) to generate the final models presented in this work. Finally, all models were evaluated in terms of their structural quality using the QMEAN³⁰ tool freely available on SWISS-MODEL.²⁵

All structures and models shown in this work were visualized using Pymol (The PyMOL Molecular Graphics System, Version 2.0 Schrödinger, LLC) and Discovery Studio® Visualizer (BIOVIA, Dassault Systèmes Discovery Studio Modeling Environment, Release 2017). In all cases, the files were saved in the Protein Data Bank (PDB) format.

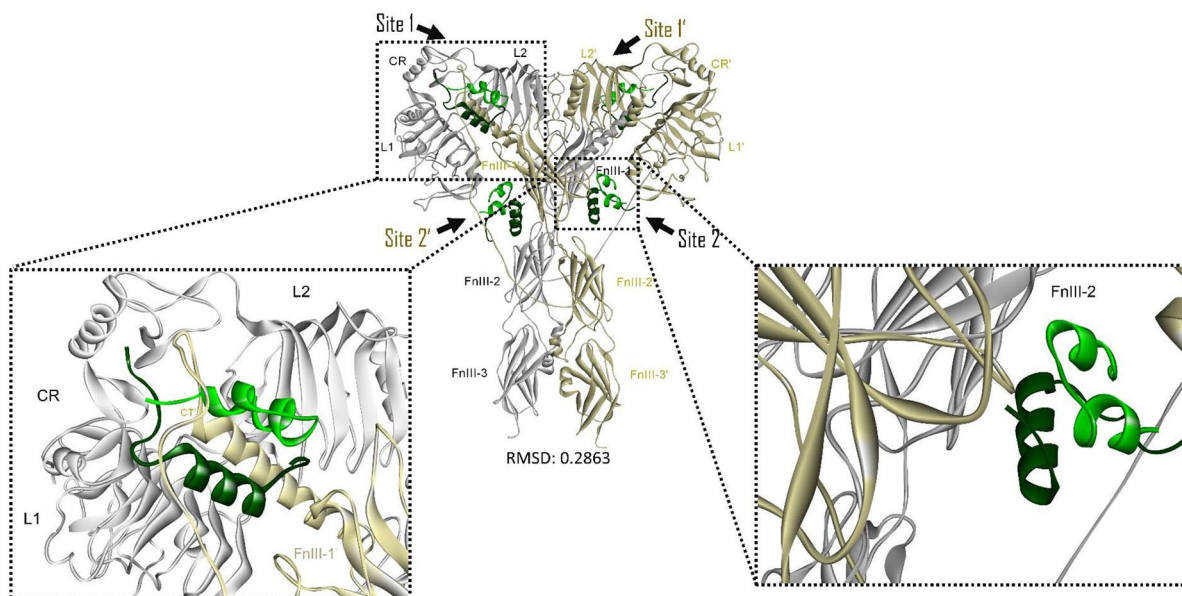


Figure 1. Metabolite M1/IR model. IR ectodomain bound to four insulin molecules (center). Enlarged images of ligand binding site 1 (left) and ligand binding site 2 (right) are shown. Metabolite M1 is in green (A chain in light green; B chain in dark green). The two IR alpha subunits are in different colors: gray (α) and golden (α'). The apostrophe (') indicates a site or domain in the IR α' -subunit. In site 1, metabolite M1 is in close contact with L1, CR, and FnIII-1' domains of IR; in site 2, metabolite M1 makes contact with the FnIII-1 domain of IR. The quality parameters for this model are: GMQE of 0.73 (high precision between 0 and 1), QMEAN score of -1.57 (good quality score closer to 0, bad quality closer to -4), and RMSD of 0.29 Å (high similarity between 0 and 2 Å).

GMQE indicates Global Model Quality Estimate; IR, insulin receptor; QMEAN, Qualitative Model Energy Analysis; RMSD, root mean square deviation.

Interaction surfaces analysis

The ligand/receptor interaction surfaces were analyzed using Discovery Studio® Visualizer software (BIOVIA, Dassault Systèmes Discovery Studio Modeling Environment, Release 2017), which was fed with each model in the PDB format.

Interaction affinities

The interaction affinities expressed as dissociation constants (Kd) were calculated using PROtein binDIng enerGY prediction (PRODIGY).^{31,32} Briefly, each model (in the PDB format) was uploaded to the web server, and chains involved in the ligand/receptor interaction were selected. A standard temperature of 25 °C was used in all the cases.

Results

Ligand/IR models

First, we modeled the structures of the metabolite M1/IR and glargine/IR complexes. The metabolite M1/IR model shows the receptor in a symmetric T-shaped conformation with four ligand molecules occupying the two high-affinity sites (sites 1 and 1') and the two low-affinity sites (sites 2 and 2') (Figure 1). A similar structure was observed in the glargine/IR model, with the receptor in a symmetric conformation with four IR-bound ligands (Supplementary Material, Figure S3).

The interaction surfaces of these two models were then analyzed, and the results are shown in Figure 2. Regarding the metabolite M1/IR model (Figure 2A), interactions were

observed between residues of the L1 (Asp12, Asp14, Leu37, Phe39), FnIII-1' (Arg498, Asn541), and α CT (Asn711, Phe714, Pro716) domains of IR, and the ligand residues (Ile^{A2}, Cys^{A7}, Tyr^{A19}, His^{B10}, Glu^{B13}, Leu^{B15}, Tyr^{B16}, Phe^{B25}, Tyr^{B26}). Some of these interactions are Ile^{A2}/Asn711, Cys^{A7}/Arg498, Leu^{B15}/Phe714, Tyr^{B16}/Phe39, Phe^{B24}/Leu37, Phe^{B25}/Arg14, and Tyr^{B26}/Asp12 (Figure 2A). A complete list of interacting residues in the metabolite M1/IR model is shown in Table 1. Regarding the interaction surface of the glargine/IR model, many interactions were found to be identical to those found in the metabolite M1/IR model; however, three unique interactions were found in the glargine/IR model (Phe^{B25}-Arg717 [hydrophobic], Arg^{B31}-Arg717 [hydrogen bond], and Asn^{A18}-Arg717 [hydrogen bond]) (Figure 2B). Since glargine contains two additional residues at the C-terminus of its B-chain (Arg^{B31} and Arg^{B32}) compared to metabolite M1, we investigated the location of these two residues in our glargine/IR model. Figure 2C shows that these two arginine residues fall into a hydrophilic region formed by the α CT and CR domains of IR, close to residues Arg270, Arg271, Gln272 (CR domain), and Arg717 (α CT domain) of IR. Table 2 shows a complete list of interacting residues in our glargine/IR model.

To validate these results, the same procedure was applied to build a model of a known structure; for this purpose, we chose to model the insulin/IR complex.²⁶ Figure 3 shows our insulin/IR computational model, in which the receptor is in a symmetrical T-shaped conformation with its four ligand-binding sites fully occupied by insulin (Figure 3, left). The

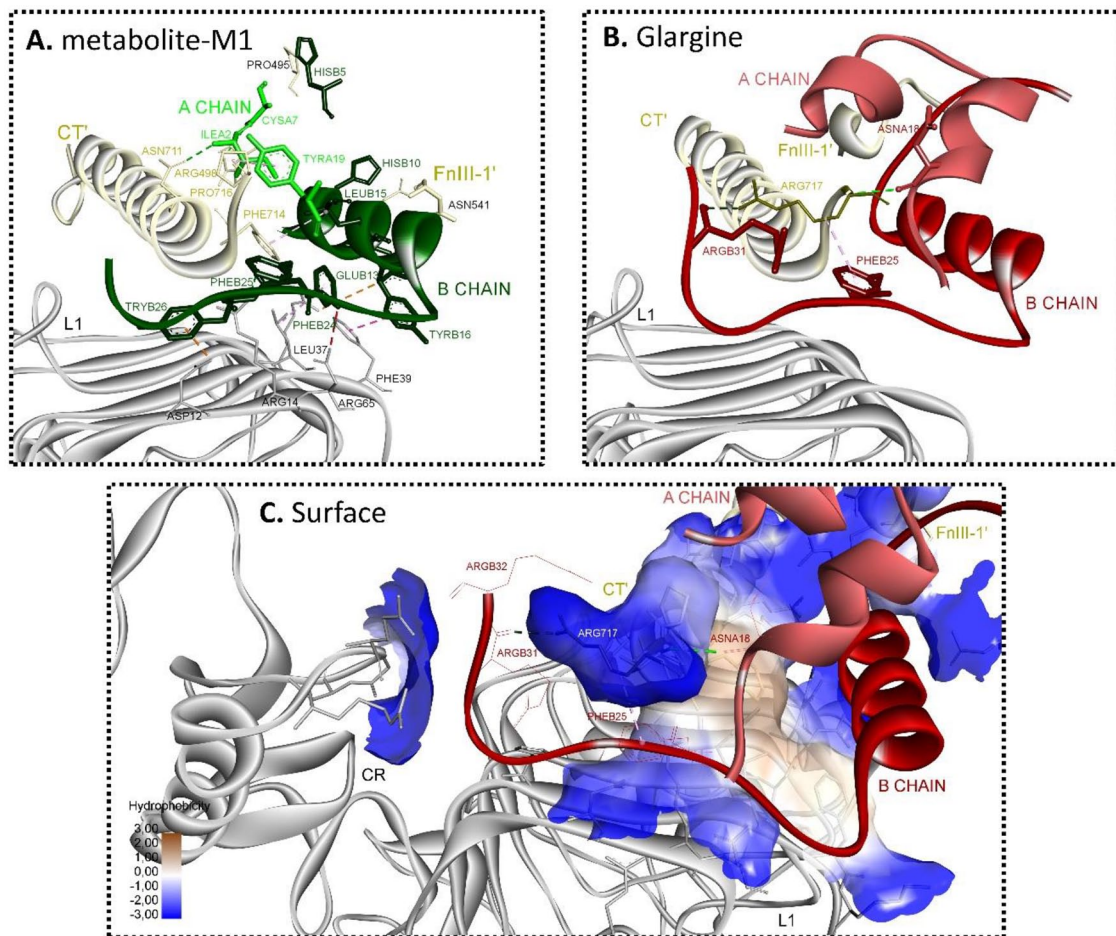


Figure 2. Contact surfaces of metabolite M1 and glargine-bound IR models. (A) Metabolite M1/IR model, with the ligand (metabolite M1) shown in green (A chain in light green; B chain in dark green). (B) Glargine/IR model, with the ligand (glargine) in red (A chain in light red; B chain in dark red). The IR alpha subunits are in gray (α) and golden (α'). Apostrophe (') indicates a site or domain in the IR α' -subunit. (C) Glargine/IR model contact surface shown with hydrophobic regions in brown color and hydrophilic regions in blue color. IR indicates insulin receptor.

Table 1. Interacting residues of metabolite M1/IR model.

LIGAND	RECEPTOR ^A
<i>A chain:</i>	α CT:
IleA2, AsnA18, TyrA19	Asn711, Pro716
	<i>FnIII-1:</i>
CysA7	Arg498
<i>B chain:</i>	α CT:
LeuB15	Phe714
	<i>FnIII-1:</i>
HisB5, HisB10	Pro495, Asn541
	<i>L1:</i>
GluB13, TyrB16, PheB24, PheB25, TyrB26	Asp12, Arg14, Leu37, Phe39, Arg65

Abbreviation: IR, insulin receptor.

^AResults for ligand binding site 1 (high affinity site). α CT, *FnIII-1*, and *L1* refer to IR domains.

Table 2. Interacting residues of glargine/IR model.

LIGAND (GLARGINE)	RECEPTOR ^A
<i>A chain:</i>	α CT:
IleA2, AsnA18, TyrA19	Asn711, Pro716, Arg717
	<i>FnIII-1:</i>
CysA7	Arg498
<i>B chain:</i>	α CT:
LeuB15, PheB25, ArgB31	Phe714, Arg717
	<i>FnIII-1:</i>
HisB5, HisB10	Pro495, Asn541
	<i>L1:</i>
GluB13, TyrB16, PheB24, PheB25, TyrB26	Asp12, Arg14, Leu37, Phe39, Arg65

Abbreviation: IR, insulin receptor.

^AResults for ligand binding site 1 (high affinity site). α CT, *FnIII-1*, and *L1* refer to IR domains.

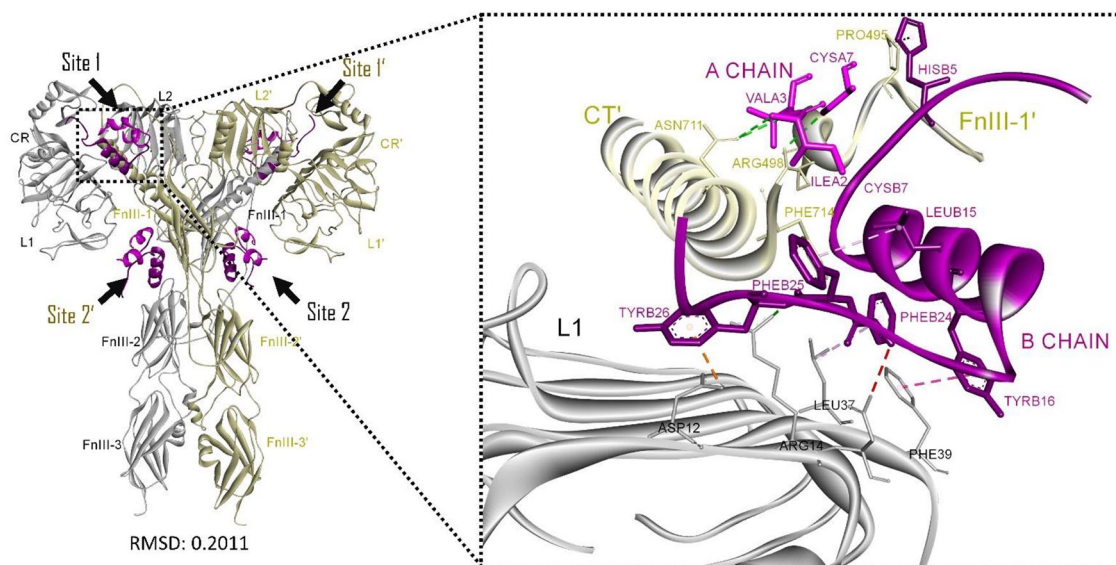


Figure 3. Insulin/IR model. Left: IR ectodomain bound to four ligand (insulin) molecules. Right: enlargement of ligand binding site 1. Insulin is shown in purple color (A chain in light purple; B chain in dark purple). The IR alpha subunits are in gray (α) and golden (α'). Apostrophe (') indicates a site or domain in the IR α' -subunit. The quality parameters for this model are: GMQE of 0.73 (high precision between 0 and 1), QMEAN score of -1.49 (good quality score closer to 0, bad quality closer to -4), and RMSD of 0.20 Å (high similarity between 0 and 2 Å). GMQE indicates Global Model Quality Estimate; IR, insulin receptor; QMEAN, Qualitative Model Energy Analysis; RMSD, root mean square deviation.

analysis of this insulin/IR model revealed 12 interactions (Ile^{A2}/Asn711, Val^{A3}/Asn711, Cys^{A7}/Arg498, His^{B5}/Pro495, His^{B10}/Asn541, Glu^{B13}/Arg65, Leu^{B15}/Phe714, Tyr^{B16}/Phe39, Phe^{B24}/Leu37, Phe^{B25}/Arg14, Tyr^{B26}/Asp12, and Thr^{B30}/Arg270) [Figure 3, right]. A multipartite interaction surface was observed: (a) the disulfide-bonded residues (Cys^{A7}-Cys^{B7}) and His^{B5} of insulin pack against Pro495, Phe497, and Arg498 in the FnIII-1' domain of IR; (b) the IR α CT residues His710 and Phe714 fit into hydrophobic pockets formed by residues Gly^{A1}, Ile^{A2}, Val^{A3}, Tyr^{A19}, Gly^{B8}, Ser^{B9}, Leu^{B11}, Val^{B12}, and Leu^{B15} of insulin; (c) the hydrophobic triad Phe^{B24}, Phe^{B25}, and Tyr^{B26} of the ligand fit into pockets formed by the amino acids Phe714, Val715, Pro718 (α CT domain), Arg14, Asn15, Leu37, and Phe39 (L1 domain) of IR. These data validate our results.

Ligand/IGF1R models

Next, we tried to model the IGF1R receptor in complex with the same ligands using the cryo-EM structure of the insulin-bound IGF1R ectodomain as a template (PDB: 6JK8).²⁸ However, with this template, only the metabolite M1/IGF1R model could be obtained (Supplementary Material, Figure S4). In this model, the IGF1R receptor shows an asymmetric Γ -shaped structure with a single ligand molecule (IGF1) bound to it. All our attempts to model the glargine/IGF1R complex were unsuccessful. Because of this difficulty and based on the structural and functional homology between IGF1R and IR, we hypothesized that this complex could possibly be modeled by assuming the IGF1R in a symmetric T-shaped conformation similar to that described for IR in our ligand/IR models. Therefore, we used another template, the insulin-bound IR

cryo-EM structure (PDB: 6PXV),²⁶ and obtained a new set of models. Figure 4 shows our new metabolite M1/IGF1R model, in which the receptor is seen in a maximally occupied symmetric T-shaped conformation with four ligand molecules bound to it, as described previously for our IR models. A similar overall structure was observed in our glargine/IGF1R model, which also showed four ligand-bound molecules (Supplementary Material, Figure S5).

Further analysis indicated that these two models share a common interaction surface, where residues of the IGF1R L1 domain (Asp8, Arg10, Tyr28, and Leu33) interact with the triad Phe^{B24}, Phe^{B25}, and Tyr^{B26} in metabolite M1 and glargine, and residues Asn698 and Phe701 of α CT interact with Ile^{A2} and Leu^{B15} (in both cases). Some of these interactions are shown in Figure 5A, which corresponds to the interaction surface of the metabolite M1/IGF1R model. A full list of the interacting residues in this model is presented in Table 3. The main difference between these two models involves the interaction of Arg^{B31} and Arg^{B32} with Glu264 and Glu305 in the CR domain of IGF1R in our glargine/IGF1R model (Figure 5B), which is missing in the metabolite M1 model. A list of interacting residues in the glargine/IGF1R symmetric model is presented in Table 4.

Discussion

In this study, bioinformatics tools were applied to obtain predictive 3D structural models of the drug/receptor complexes between glargine (or its metabolite M1) and the IR and IGF1R receptors. None of these structures have been reported in the databases. Homology modeling was performed using the SWISS-MODEL server.²⁵

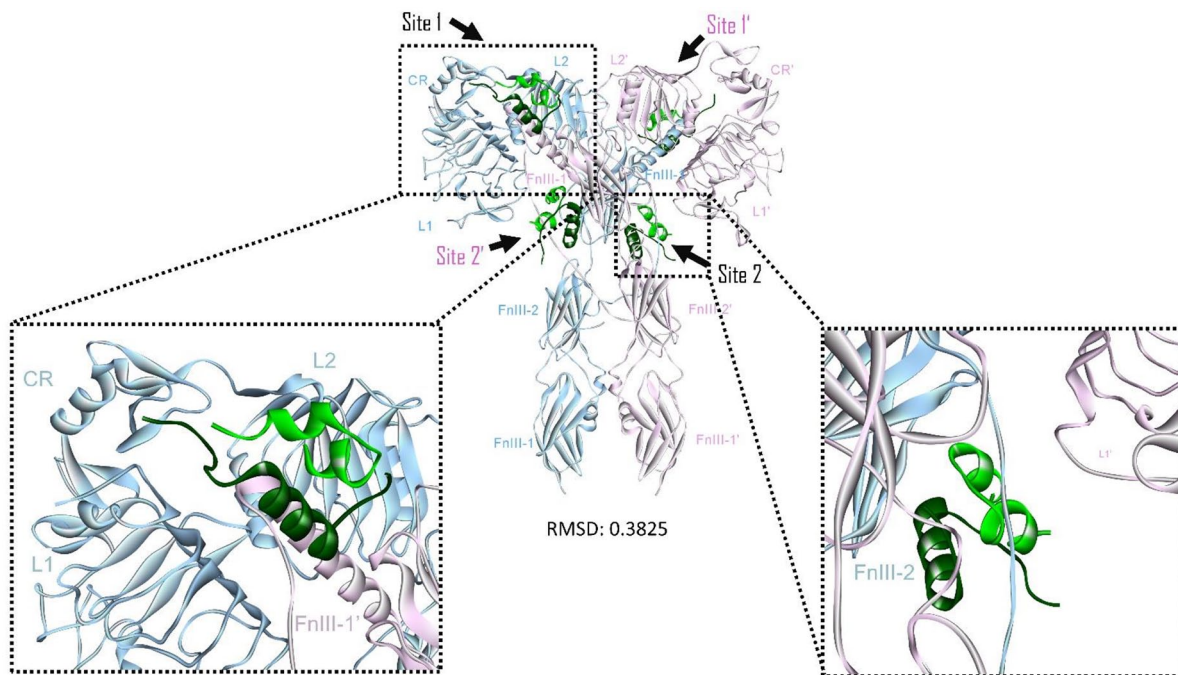


Figure 4. Metabolite M1/IGF1R symmetric model. Center: IGF1R bound to four ligand (metabolite M1) molecules. Lower left: expanded view of the ligand binding site 1, where glargine M1 is seen in close contact with the IGF1R domains L1, CR, and FnIII-1'. Lower right: expanded view of the ligand binding site 2, where glargine M1 makes contact with the IGF1R domain FnIII-1. Metabolite M1 is shown in green (A chain in light green; B chain in dark green). IGF1R alpha subunits are colored blue (α) and lavender (α'). Apostrophe (') indicates a site or domain in the IR α' -subunit. The quality parameters for this model are: GMQE of 0.77 (high precision between 0 and 1), QMEAN score of -2.91 (good quality closer to 0, bad quality closer to -4), and RMSD of 0.35 Å (high similarity between 0 and 2 Å).
GMQE indicates Global Model Quality Estimate; IGF1R, insulin-like growth factor type 1 receptor; QMEAN, Qualitative Model Energy Analysis; RMSD, root mean square deviation.

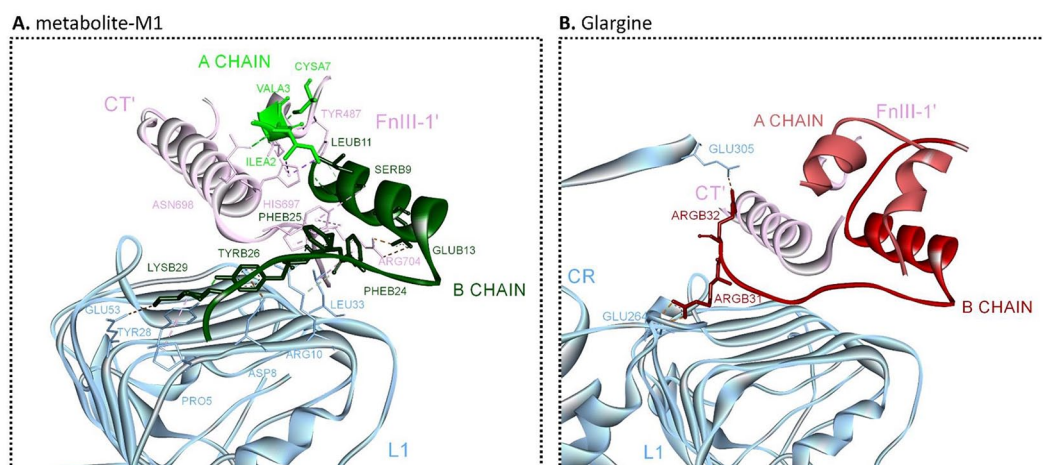


Figure 5. Contact surfaces of metabolite M1 and glargine-bound IGF1R symmetric models. (A) Metabolite M1/IGF1R model, where the metabolite M1 is shown in green (A chain in light green; B chain in dark green). (B) Glargine/IGF1R model, with glargine shown in red (A chain in light red; B chain in dark red). Receptor residues and structure are colored blue (α) and lavender (α'). Apostrophe (') indicates a site or domain in the IR α' -subunit. IGF1R indicates insulin-like growth factor type 1 receptor.

Concerning the drug/IR complexes, the cryo-EM structure of the fully liganded insulin/IR (ectodomain) was used as a template for modeling. The IR ectodomain in this template shows a symmetrical T-shaped conformation.²⁶ Consequently, a symmetrical IR conformation and full receptor occupation (four receptor-bound ligand molecules) were also observed in our models. As for the interaction surface, several interactions

in our drug/IR models (glargine/IR and metabolite M1/IR) have also been reported in the insulin/IR structures obtained by X-ray crystallography and cryo-EM.^{26,33,34} Among these interactions are the following: (a) Ile^{A2} and Leu^{B15} (ligand) with Asn⁷¹¹ and Phe⁷¹⁴, respectively (IR, segment α CT); (b) His^{B5}, Cys^{A7}, and His^{B10} (ligand) with Pro⁴⁹⁵, Arg⁴⁹⁸, and Asn⁵⁴¹, respectively (IR, domain FnIII-1); and (c) Tyr^{B26},

Table 3. Interacting residues of metabolite M1/IGF1R model (symmetric conformation).

LIGAND	RECEPTOR (IGF1R) ^a
<i>A chain:</i>	<i>αCT:</i>
IleA2, ValA3	His697, Asn698
	<i>FnIII-1:</i>
CysA7	Arg488
<i>B chain:</i>	<i>L1:</i>
PheB24, PheB25, TyrB26, LysB29	Pro5, Asp8, Arg10, Tyr28, Leu33, Glu53
	<i>αCT:</i>
LeuB11, ValB12, GluB13, LeuB15	His697, Phe701, Pro703, Arg704
	<i>FnIII-1:</i>
SerB9	Tyr487

Abbreviation: IGF1R, insulin-like growth factor type 1 receptor.

^aResults for ligand binding site 1 (high affinity site). *αCT*, *FnIII-1*, and *L1* refer to IGF1R domains.

Phe^{B24}, and Tyr^{B16} (ligand) with Asp12, Leu37, and Phe39, respectively (IR, domain L1). All these interactions are important for insulin/IR binding.³³⁻³⁵ A novel finding in our work is related to the interactions observed in the glargine/IR model, specifically those involving residues Arg^{B31} and Arg^{B32} at the C-terminus of the glargine B-chain. We found that these two arginine residues fall into a hydrophilic region formed by the *αCT* and CR domains of IR, close to residues Arg270, Arg271, and Gln272 (CR domain), and Arg717 (*αCT* domain) of IR. Specific interactions observed in this region were Phe^{B25}/Arg717, Arg^{B31}/Arg717, and AsnA18/Arg717, and none of these interactions have been previously reported. Our results agree with the predictions of other authors, suggesting that Arg^{B31} and Arg^{B32} participate in glargine/IR interaction.^{15,36}

Although we cannot rule out the possibility that these results represent an erroneous finding, it should be kept in mind that unlike insulin and metabolite M1, the binding of glargine to IR involves accommodating two additional arginine residues (Arg^{B31} and Arg^{B32}) belonging to the glargine B-chain C-terminus. These two amino acids should be accommodated in a hydrophilic cavity close to the aromatic triad Phe^{B24}, Phe^{B25}, and Tyr^{B26} of insulin that interact with the receptor residues Phe39 (L1 domain), Phe714, Val715, and Pro718 (*αCT* segment) in the insulin binding site, which has been described by other authors.^{33,34} Our model reveals a possible hydrophilic region proximal to the hydrophobic portion of the ligand binding site, where Arg717 (*αCT*) is located and interacts with glargine via hydrogen bonding and hydrophobic interactions. Therefore, we believe that our findings are plausible, and our model provides a hypothetical structural basis for the involvement of those arginine residues in glargine/receptor

Table 4. Interacting residues of glargine/IGF1R model (symmetric conformation).

LIGAND	RECEPTOR ^a
<i>A Chain:</i>	<i>αCT:</i>
IleA2, TyrA19	Asn698, Pro703
	<i>FnIII-1</i>
CysA7	Arg488
<i>B CHAIN:</i>	<i>L1</i>
GluB13, TyrB16, PheB24, PheB25, TyrB26	Asp8, Arg10, Tyr28, Leu33, Ser35, Arg59
	<i>CR</i>
LysB29, ArgB31, ArgB32,	Asp262, Glu264, Glu305
	<i>αCT</i>
LeuB15	Phe701
	<i>FnIII-1</i>
HisB5, SerB9	Pro485, Tyr487

Abbreviation: IGF1R, insulin-like growth factor type 1 receptor.

^aResults for ligand binding site 1 (high affinity site). *αCT*, *FnIII-1*, and *L1* refer to IGF1R domains.

interactions. Further experimental work is needed to confirm or rule out this possibility, and our glargine/IR model is a starting point toward this goal.

Regarding IGF1R, we tried to obtain the glargine/IGF1R model by following the same procedure, but it did not work when we used the cryo-EM structure of the insulin-bound IGF1R ectodomain as a template.²⁸ However, this difficulty was overcome when we considered the possibility that this receptor could exhibit a symmetric conformation similar to that described for IR in full occupancy by insulin. Therefore, by using a different modeling template, we obtained new models showing a symmetric T-shaped conformation, full occupation with four ligand molecules bound to IGF1R, and a high overall similarity among them (glargine vs metabolite M1) and to the drug/IR models. Interestingly, our glargine/IGF1R model revealed new interactions involving the glargine residues Arg^{B31} and Arg^{B32}, and the IGF1R residues Glu294 and Glu335. The involvement of glargine residues Arg^{B31} and Arg^{B32} in interaction with this receptor has been suggested by other authors,^{15,36} although no specific interactions have thus far been described. This result with glargine/IGF1R also represents novel findings. Regarding our hypothesis that IGF1R could assume a symmetric T-shaped conformation similar to that described for IR,²⁶ it is only supported by the fact that both receptors share a high functional and structural identity (58% sequence identity). We do not have experimental support for this conformation, but different studies indicate that the current model of IGF1R function with two conformational states (active vs inactive) is too simplistic and does not represent reality.³⁷

Thus, we speculate that IGF1R could fluctuate between alternate conformations with differential degrees of activity depending on their occupation. In this way, the unoccupied receptor would represent an inactive conformation and binding of a single ligand molecule would induce a partially active asymmetric conformation, whereas binding of four ligand molecules would induce the fully occupied symmetric conformation. This is similar to the recently suggested IR activation mechanism.²⁶ Thus far, however, the active receptor is considered as a Γ -shaped asymmetric IGF1R dimer with a single molecule of ligand bound to it.²⁸

Regarding the insulin/IR complex, it is known that insulin changes its conformation after binding to IR, with major changes in the C-terminal tail of the insulin B chain, where a reorientation of the B20-28 segment occurs, followed by a 60° rotation of the B25-28 portion.^{5,34,35,38} This conformational change moves some residues away from the insulin molecule core, exposing the non-polar side chains of some residues from both the A and B chains (Ile^{A2}, Val^{A3}, Val^{B12}, Phe^{B24}, and Phe^{B25}).^{5,34,35,38} Thus, in the insulin/IR system, there is a clear structural difference between the bound and unbound conformations of insulin at the C-end tail of the B chain. Interestingly, a similar arrangement of the C-terminal tail of the B chain was observed in our models of glargine and metabolite M1 with both receptors (results not shown), suggesting that similar conformational changes would occur by the binding of glargine and metabolite M1 to both receptors (IR and IGF1R).

Although no crystallographic or cryo-EM data have been reported so far for these glargine-bound receptors, experimental data on binding affinities are available for all the complexes studied here. In this regard, Sommerfeld et al³⁹ reported that glargine and metabolite-M1 bind to IR with affinities of 1.10 and 1.35 nM, and to IGF1R with affinities of 63 and 649 nM, respectively. With the same ligands, Werner et al⁴⁰ reported binding affinities of 5.2 and 6.4 nM for IR, and 20.3 and 645 nM for IGF1R, respectively. Theoretical affinities (Kd) of our models with IR were 2.0 nM (glargine/IR) and 6.2 nM (metabolite M1/IR), while those of our IGF1R models were 1.3 nM (glargine/IGF1R) and 28.0 nM (metabolite M1/IGF1R) (not shown). Therefore, our theoretical results agree well with experimental reports by other authors not only in terms of the magnitude of binding affinities, but also in the fact that glargine shows a higher binding affinity to both receptors. It is also noteworthy that when we applied the same predictive procedure to a system whose 3D structure was already known (insulin bound to IR), the theoretical model correlated well with the experimental one, which validates our procedure and our study.

In this study, bioinformatics tools were applied to obtain predictive models and to analyze the hypothetical ligand-receptor interactions in the system formed by IR and IGF1R, and their ligands glargine and metabolite M1. To the best of

our knowledge, our study is the first to provide an insight, at least from a theoretical predictive point of view, on the structural basis of drug-receptor interactions involving glargine and the receptors IR and IGF1R, opening new avenues in this field. Currently, the issue of protein structure prediction is very relevant because of the gap that exists between the rate of appearance of new sequences and the elucidation of new protein structures in databases.⁴¹ We followed a template-based approach, which compares the amino acid sequence of a protein whose structure is unknown (target sequence) with one or more sequences from homologous proteins of known structures (templates) to build a 3D model based on this homology.⁴² Among the different classical methods, the homology modeling approach is the most reliable and accurate for sequences with high homology, as seen in our case.⁴¹ This approach is very simple to carry out for monomeric proteins; but in more complex systems such as the one studied here, where the receptor and the ligand each have two peptide chains and are also disulfide-bonded, the procedure is more complicated and requires greater understanding. Therefore, we believe that this work is relevant not only from a scientific point of view but also from an educational perspective, and our procedure could be useful for teaching more complex models in bioinformatics, molecular pharmacology, and/or biochemistry courses.

In conclusion, our work shows the application of bioinformatics tools to obtain predictive models and provides a better understanding of the drug/receptor interactions involving glargine, its metabolite M1, and the IR and IGF1R receptors.

Acknowledgements

We thank the Universidad Nacional de Colombia, Facultad de Ciencias, and Departamento de Farmacia for providing the time, resources, and physical facilities for the development of this work. We would like to thank Editage (www.editage.com) for English language editing.

Author Contributions

M.G.-B. conducted all *in silico* analysis and wrote the paper. C.G.-A. performed the research design and wrote the paper.

Disclaimers

The views expressed in the submitted article are the authors' own and not an official position of the Universidad Nacional de Colombia.

ORCID iD

Claudio Gómez-Alegría  <https://orcid.org/0000-0003-4572-4283>

Supplemental Material

Supplemental material for this article is available online.

REFERENCES

- Chang L, Chiang SH, Saltiel AR. Insulin signaling and the regulation of glucose transport. *Mol Med*. 2004;10:65-71. doi:10.2119/2005-00029.Saltiel.
- Saltiel AR, Kahn CR. Insulin signalling and the regulation of glucose and lipid metabolism. *Nature*. 2001;414:799-806. doi:10.1038/414799a.
- De Meyts P. Insulin and its receptor: structure, function and evolution. *Bioessays*. 2004;26:1351-1362. doi:10.1002/bies.20151.
- Ward CW, Menting JG, Lawrence MC. The insulin receptor changes conformation in unforeseen ways on ligand binding: sharpening the picture of insulin receptor activation. *Bioessays*. 2013;35:945-954. doi:10.1002/bies.201300065.
- Hua Q. Insulin: a small protein with a long journey. *Protein Cell*. 2010;1:537-551. doi:10.1007/s13238-010-0069-z.
- Rosenstock J, Guerci B, Hanefeld M, et al. Prandial options to advance basal insulin glargine therapy: testing lixisenatide plus basal insulin versus insulin glulisine either as basal-plus or basal-bolus in type 2 diabetes: the GetGoal Duo-2 Trial. *Diabetes Care*. 2016;39:1318-1328. doi:10.2337/dc16-0014.
- Sciaccia L, Vella V, Frittitta L, et al. Long-acting insulin analogs and cancer. *Nutr Metab Cardiovasc Dis*. 2018;28:436-443. doi:10.1016/j.numecd.2018.02.010.
- Sheldon B, Russell-Jones D, Wright J. Insulin analogues: an example of applied medical science. *Diabetes Obes Metab*. 2009;11:5-19. doi:10.1111/j.1463-1326.2008.01015.x.
- Lucidi P, Porcellati F, Yki-Järvinen H, et al. Low levels of unmodified insulin glargine in plasma of people with type 2 diabetes requiring high doses of basal insulin. *Diabetes Care*. 2015;38:e96-e97. doi:10.2337/dc14-2662.
- Hilgenfeld R, Seipke G, Berchtold H, Owens DR. The evolution of insulin glargine and its continuing contribution to diabetes care. *Drugs*. 2014;74:911-927. doi:10.1007/s40265-014-0226-4.
- Agin A, Jeandidier N, Gasser F, Grucker D, Sapin R. Glargine blood biotransformation: in vitro appraisal with human insulin immunoassay. *Diabetes Metab*. 2007;33:205-212. doi:10.1016/j.diabet.2006.12.002.
- Bolli GB, Hahn AD, Schmidt R, et al. Plasma exposure to insulin glargine and its metabolites M1 and M2 after subcutaneous injection of therapeutic and supratherapeutic doses of glargine in subjects with type 1 diabetes. *Diabetes Care*. 2012;35:2626-2630. doi:10.2337/dc12-0270.
- Liu S, Li Y, Lin T, Fan X, Liang Y, Heemann U. High dose human insulin and insulin glargine promote T24 bladder cancer cell proliferation via PI3K-independent activation of Akt. *Diabetes Res Clin Pract*. 2011;91:177-182. doi:10.1016/j.diabres.2010.11.009.
- Tennagels N, Werner U. The metabolic and mitogenic properties of basal insulin analogues. *Arch Physiol Biochem*. 2013;119:1-14. doi:10.3109/13813455.2012.754474.
- Varewijck AJ, Janssen JA. Insulin and its analogues and their affinities for the IGF1 receptor. *Endocr Relat Cancer*. 2012;19:F63-F75. doi:10.1530/ERC-12-0026.
- Vigneri R, Squatrito S, Sciaccia L. Insulin and its analogs: actions via insulin and IGF receptors. *Acta Diabetol*. 2010;47:271-278. doi:10.1007/s00592-010-0215-3.
- Wu JW, Azoulay L, Majdan A, Boivin JF, Pollak M, Suissa S. Long-term use of long-acting insulin analogs and breast cancer incidence in women with type 2 diabetes. *J Clin Oncol*. 2017;35:3647-3653. doi:10.1200/JCO.2017.73.4491.
- Mori Y, Ko E, Furrer R, et al. Effects of insulin and analogues on carcinogen-induced mammary tumours in high-fat-fed rats. *Endocr Connect*. 2018;7:739-748. doi:10.1530/EC-17-0358.
- Lemmon MA, Schlessinger J. Cell signaling by receptor tyrosine kinases. *Cell*. 2010;141:1117-1134. doi:10.1016/j.cell.2010.06.011.
- De Meyts P. The insulin receptor: a prototype for dimeric, allosteric membrane receptors? *Trends Biochem Sci*. 2008;33:376-384. doi:10.1016/j.tibs.2008.06.003.
- Hausler RA, McGraw TE, Accili D. Biochemical and cellular properties of insulin receptor signalling. *Nat Rev Mol Cell Biol*. 2018;19:31-44. doi:10.1038/nrm.2017.89.
- Lawrence MC, McKern NM, Ward CW. Insulin receptor structure and its implications for the IGF-1 receptor. *Curr Opin Struct Biol*. 2007;17:699-705. doi:10.1016/j.sbi.2007.07.007.
- De Meyts P, Whittaker J. Structural biology of insulin and IGF1 receptors: implications for drug design. *Nat Rev Drug Discov*. 2002;1:769-783. doi:10.1038/nrd917.
- Lipska KJ. Insulin analogues for type 2 diabetes. *JAMA*. 2019;321:350-351. doi:10.1001/jama.2018.21356.
- Waterhouse A, Bertoni M, Bienert S, et al. SWISS-MODEL: homology modelling of protein structures and complexes. *Nucleic Acids Res*. 2018;46:W296-W303. doi:10.1093/nar/gky427.
- Uchikawa E, Choi E, Shang G, Yu H, Bai XC. Activation mechanism of the insulin receptor revealed by cryo-EM structure of the fully liganded receptor-ligand complex. *eLife*. 2019;8:e48630. doi:10.7554/eLife.48630.
- Ratha BN, Kar RK, Bednarikova Z, et al. Molecular details of a salt bridge and its role in insulin fibrillation by NMR and Raman spectroscopic analysis. *J Phys Chem B*. 2020;124:1125-1136. doi:10.1021/acs.jpcc.9b10349.
- Zhang X, Yu D, Sun J, et al. Visualization of ligand-bound ectodomain assembly in the full-length human IGF-1 receptor by cryo-EM single-particle analysis. *Structure*. 2020;28:555-561.e4. doi:10.1016/j.str.2020.03.007.
- Berman HM, Westbrook J, Feng Z, et al. The Protein Data Bank. *Nucleic Acids Res*. 2000;28:235-242. doi:10.1093/nar/28.1.235.
- Benkert P, Biasini M, Schwede T. Toward the estimation of the absolute quality of individual protein structure models. *Bioinformatics*. 2011;27:343-350. doi:10.1093/bioinformatics/btq662.
- Vangone A, Bonvin AM. Contacts-based prediction of binding affinity in protein-protein complexes. *eLife*. 2015;4:e07454. doi:10.7554/eLife.07454.
- Xue LC, Rodrigues JP, Kastrius PL, Bonvin AM, Vangone A. PRODIGY: a web server for predicting the binding affinity of protein-protein complexes. *Bioinformatics*. 2016;32:3676-3678. doi:10.1093/bioinformatics/btw514.
- Crudden C, Shibano T, Song D, Suleymanova N, Girnita A, Girnita L. Blurring boundaries: receptor tyrosine kinases as functional G protein-coupled receptors. *Int Rev Cell Mol Biol*. 2018;339:1-40. doi:10.1016/bs.ircmb.2018.02.006.
- Menting JG, Whittaker J, Margetts MB, et al. How insulin engages its primary binding site on the insulin receptor. *Nature*. 2013;493:241-245. doi:10.1038/nature11781.
- Menting JG, Yang Y, Chan SJ, et al. Protective hinge in insulin opens to enable its receptor engagement. *Proc Natl Acad Sci USA*. 2014;111:E3395-E3404. doi:10.1073/pnas.1412897111.
- Weis F, Menting JG, Margetts MB, et al. The signalling conformation of the insulin receptor ectodomain. *Nat Commun*. 2018;9:4420. doi:10.1038/s41467-018-06826-6.
- Sliker LJ, Brooke GS, DiMarchi RD, et al. Modifications in the B10 and B26-30 regions of the B chain of human insulin alter affinity for the human IGF-I receptor more than for the insulin receptor. *Diabetologia*. 1997;40:S54-S61. doi:10.1007/s001250051402.
- Derewenda U, Derewenda Z, Dodson EJ, Dodson GG, Bing X, Markussen J. X-ray analysis of the single chain B29-A1 peptide-linked insulin molecule. A completely inactive analogue. *J Mol Biol*. 1991;220:425-433. doi:10.1016/0022-2836(91)90022-x.
- Sommerfeld MR, Müller G, Tschank G, et al. In vitro metabolic and mitogenic signaling of insulin glargine and its metabolites. *PLoS ONE*. 2010;5:e9540. doi:10.1371/journal.pone.0009540.
- Werner U, Korn M, Schmidt R, Wendrich TM, Tennagels N. Metabolic effect and receptor signalling profile of a non-metabolisable insulin glargine analogue. *Arch Physiol Biochem*. 2014;120:158-165. doi:10.3109/13813455.2014.950589.
- Jisna VA, Jayaraj PB. Protein structure prediction: conventional and deep learning perspectives. *Protein J*. 2021;40:522-544. doi:10.1007/s10930-021-10003-y.
- Lam SD, Das S, Sillitoe I, Orengo C. An overview of comparative modelling and resources dedicated to large-scale modelling of genome sequences. *Acta Crystallogr D Struct Biol*. 2017;73:628-640. doi:10.1107/S2059798317008920.